School of Medicine Publications and Presentations

School of Medicine

9-21-2018

Magnolin targeting of ERK1/2 inhibits cell proliferation and colony growth by induction of cellular senescence in ovarian cancer cells

Ji-Hong Song

Cheol-Jung Lee

Hyun-Jung An

Sun-Mi Yoo

Han C. Kang

See next page for additional authors

Authors

Ji-Hong Song, Cheol-Jung Lee, Hyun-Jung An, Sun-Mi Yoo, Han C. Kang, Joo Y. Lee, Kwang D. Kim, Dae Joon Kim, Hye S. Lee, and Yong-Yeon Cho

RESEARCH ARTICLE

WILEY Molecular Carcinogenesis

Magnolin targeting of ERK1/2 inhibits cell proliferation and colony growth by induction of cellular senescence in ovarian cancer cells

Ji-Hong Song[1] │ Cheol-Jung Lee[1] │ Hyun-Jung An[1] │ Sun-Mi Yoo[1] │ Han C. Kang[1] │ Joo Y. Lee[1] │ Kwang D. Kim[2] │ Dae J. Kim[3] │ Hye S. Lee[1] │ Yong-Yeon Cho[1] (iD)

[1] Integrated Research Institute of Pharmaceutical Sciences, BK21 PLUS Team & BRL, College of Pharmacy, The Catholic University of Korea, Wonmi-gu, Bucheon-si, Gyeonggi-do, Korea

[2] Division of Applied Life Science (BK21 Plus), PMBBRC, Gyeongsang National University, Jinju-daero, Jinju-si, Gyeongsangnam-do, Korea

[3] Department of Biomedical Sciences, School of Medicine, University of Texas Rio Grande Valley, Texas

Correspondence
Yong-Yeon Cho, PhD and Hye Suk Lee, PhD, College of Pharmacy, The Catholic University of Korea, 43, Jibong-ro, Wonmi-gu, Bucheon-si, Gyeonggi-do 14662, Republic of Korea.
E-mails: yongyeon@catholic.ac.kr (Y.Y.C.), sianalee@catholic.ac.kr (H.S.L.)

Funding information
Catholic University of Korea, Grant number: M-2018-B0002-00011; National Research Foundation of Korea, Grant numbers: NRF-2017M3A9F5028608, NRF-2017R1A2B2002012, NRF-2017R1A4A1015036, NRF-22A20130012250

Ras/Raf/MEKs/ERKs and PI3 K/Akt/mTOR signaling pathways have key roles in cancer development and growth processes, as well as in cancer malignance and chemo-resistance. In this study, we screened the therapeutic potential of magnolin using 15 human cancer cell lines and combined magnolin sensitivity with the CCLE mutaome analysis for relevant mutation information. The results showed that magnolin efficacy on cell proliferation inhibition were lower in TOV-112D ovarian cancer cells than that in SKOV3 cells by G1 and G2/M cell cycle phase accumulation. Notably, magnolin suppressed colony growth of TOV-112D cells in soft agar, whereas colony growth of SKOV3 cells in soft agar was not affected by magnolin treatment. Interestingly, phospho-protein profiles in the MAPK and PI3 K signaling pathways indicated that SKOV3 cells showed marked increase of Akt phosphorylation at Thr308 and Ser473 and very weak ERK1/2 phosphorylation levels by EGF stimulation. The phospho-protein profiles in TOV-112D cells were the opposite of those of SKOV3 cells. Importantly, magnolin treatment suppressed phosphorylation of RSKs in TOV-112D, but not in SKOV3 cells. Moreover, magnolin increased SA-β-galactosidase-positive cells in a dose-dependent manner in TOV-112D cells, but not in SKOV3 cells. Notably, oral administration of Shin-Yi fraction 1, which contained magnolin approximately 53%, suppressed TOV-112D cell growth in athymic nude mice by induction of $p16^{Ink4a}$ and $p27^{Kip1}$. Taken together, targeting of ERK1 and ERK2 is suitable for the treatment of ovarian cancer cells that do not harbor the constitutive active P13 K mutation and the loss-of-function mutations of the p16 and/or p53 tumor suppressor proteins.

KEYWORDS
chemoresistance, mutaome, natural compound, signaling target

1 | INTRODUCTION

Ovarian cancer is the leading cause of death from gynecological malignancies in women. Early-stage ovarian cancer is asymptomatic, and approximately 75% of patients are already in an advanced stage of the disease when diagnosed.[1] Although recent progress in the development of anticancer drugs has led to a remarkable increase in overall survival from various malignancies, including ovarian cancer, the 5-year survival rate for patients with advanced stage ovarian cancer remains low.[2] Conventional surgery and chemotherapy-based treatment modules appear to be ineffective in reducing the mortality rate of ovarian cancer because of its recurrence frequency and resistance to chemotherapy. Gene mutations in *K-Ras*, *p53*, and/or *phosphatidylinositide 3-kinase* (*PI3 K*) are related to chemoresistance in ovarian cancers.[3] For example, *K-Ras* mutation is associated with cisplatin resistance in ovarian cancer.[4] However, mutaome-based chemoresistance mechanisms in ovarian cancer have not been clearly elucidated.

Chemoresistance may be characterized as intrinsic chemoresistance, which is involved in pharmacokinetics/pharmacodynamics by limiting drugs uptake, enhancing efflux, or activating detoxification of drugs, or extrinsic chemoresistance, which is associated with genetic or epigenetic alterations of crucial genes.[1] Genetic alterations are reflected in DNA sequences and include mutations, deletions, amplifications, and translocations, and can result in the development and/or the utilization of non-canonical signaling pathways that are not observed in normal cells.[1] Well-characterized signaling pathways involved in the controlling of cancer development and chemoresistance are the Ras/Raf/MEKs/ERKs/RSKs and PI3 K/Akt/mTOR signaling pathways, which are generally known to control cell proliferation and transformation, cell survival and death, and cell locomotion including that associated with cancer cell metastasis.[5] These features are closed related to cancer cell malignancy and chemoresistance, which are obtained via an accumulation of genomic mutations.[6] For example, mutations of K-Ras or Raf in the Ras/Raf/MEKs/ERKs/RSKs signaling pathway are frequently observed in cancer cells harboring chemoresistance against paclitaxel or doxorubicin in acute lymphoblastic leukemia, melanoma, colon, gastrointestinal, and non-small-cell lung cancer,[7,8] whereas, mutations of PI3 K in the PI3 K/Akt/mTOR signaling pathway are observed in breast cancer, head and neck squamous cell carcinoma, prostate cancer, colon cancer, and non-small-cell lung cancer and are associated with a lack of cell sensitivity to anticancer drugs.[9] Regardless, the relationships between genetic alterations and chemoresistance have not been completely described.

Recently, bioinformatic data obtained from the mutaome database of the Cancer Cell Line Encyclopedia (CCLE) provided the opportunity to investigate the relationships between chemoresistance and accumulated mutations in the cancer cells. Based on CCLE mutaome data, our research group has sought to elucidate the association of a particular mutation or signaling pathway with chemoresistance, in particular, the Ras/Raf/MEKs/ERKs/RSKs and PI3 K/Akt/mTOR signaling pathways. The data indicate that 20–80% of mutations in most tumors occur in more than one gene, and those genes often include *p53*, *PIK3*, *APC*, *PTEN*, *B-Raf*, *Ras*, and others. For example, when taxol or cisplatin is treated, A549 human lung cancer cells harboring mutations both at p53 and K-Ras produce chemoresistance.[10] Moreover, HER-positive breast cancer cells and head and neck squamous cell carcinomas those harbor mutations in PI3 K and Ras or PTEN and PI3 K are resistant to Trastuzumab (also known as Herceptin: a humanized monoclonal antibody against HER2)[11] and Cetuximab (a monoclonal blocking antibody against the epidermal growth factor receptor EGFR),[12] respectively. Therefore, although particular mutations in a genome may be clearly associated with chemoresistance, difficulties in handling of big data by researchers have become a substantial hurdle when attempting to reveal or suggest possible mechanisms related to how chemoresistance is expressed in cancer cells.

Magnolin is a lignan compound abundantly found in *Magnolia* spp. and has been widely used as an oriental medicinal herb to treat various human diseases and conditions including empyema, nasal congestion, sinusitis, and inflammation.[13] Recently, our research group reported that that magnolin is capable of suppressing cell proliferation and transformation by impairing the G1/S cell-cycle transition and inhibiting the ERKs/RSK2 signaling pathways by direct targeting of the active pockets of ERK1 and ERK2.[13] That study also showed that magnolin inhibits anchorage-independent cell transformation induced by tumor promoters such as EGF.[13] However, the biological effects of magnolin as a cancer therapeutic agent have not been fully described. In this study, we investigated the efficacy of magnolin as an inhibitor of the ERKs/RSK2 signaling axis in cancer cells, as well as the molecular mechanism associated with the magnolin resistance of SKOV3 ovarian cancer cells.

2 | MATERIALS AND METHODS

2.1 | Reagents and antibodies

Chemicals such as Tris, NaCl and sodium dodecyl sulfate (SDS) for buffer preparation were purchased from Sigma-Aldrich (St. Louis, MO). Magnolin extracted from Shin-Yi, the dried flower buds of *Magnolia biondii* (Magnolia flos), was generously provided by Dr. S.-R. Oh at the Korea Research Institute of Bioscience and Biotechnology. Cell culture media and other supplements were from Life Science Technologies (Rockville, MD) or Corning (Manassas, VA). Antibodies against p-ERK1/2 (T202/Y204), p-Akt (S473), p-Akt (T308), p-p90RSK (T359/S363), total-ERK, total-Akt, total-RSK, and total-ATF1 were from Cell Signaling Biotechnology (Beverly, MA). Antibodies against β-actin and p-ATF1 (S63) were purchased from Abcam (Cambridge, MA). Antibodies against human p16^Ink4a, p27^Kip1, and anti-rabbit and anti-mouse secondary antibodies conjugated with horseradish peroxidase were obtained from Santa Cruz Biotechnology (Santa Cruz, CA). Antibodies against CD44 and CD24 were obtained from BioLegend (San Diego, CA). The *DC* protein assay quantification kit was obtained from Bio-Rad Laboratories (Hercules, CA). Active Akt1 recombinant protein was purchased from SignalChem (Richmond, BC, Canada). The Cell Titer 96

Aqueous One Solution Reagent [3-(4,5-dimethylthiazol-2-yl)-5-(3-carboxymethoxyphenyl)-2-(4-sulfophenyl)-2H-tetrazolium, inner salt (MTS)] kit for assay of cell proliferation was from Promega (Madison, WI).

2.2 | Cell culture

Human pancreatic cancer cell lines (AsPC-1, BxPC-3, Capan-1, Capan-2, and MIA PaCa-2), human colon cancer cell lines (SW480, HCT 116, HT-29, and COLO 205), human breast cancer cell lines (MCF7, MDA-MB-231, SKBR3, and BT-474), and human ovarian cancer cell lines (TOV-112D and SKOV3) were purchased from the American Type Culture Collection (Manassas, VA). The MCF7 and TOV-112D cells were cultured in minimum essential medium (MEM) supplemented with 10% fetal bovine serum (FBS) and antibiotics (100 units each of penicillin and streptomycin). Capan-1 cells were cultured in Iscove's modification of Dulbecco's modified Eagle's medium (IDMEM) supplemented with 20% FBS and antibiotics (100 units each of penicillin and streptomycin). MIA PaCa-2 and MDA-MD-231 cells were cultured in DMEM supplemented with 10% FBS and antibiotics (100 units each of penicillin and streptomycin). SW480, COLO 205, SKBR3, BT-474, and SKOV3 cells were cultured in RPMI1640 supplemented with 10% FBS and antibiotics (100 units each of penicillin and streptomycin). All cells were maintained at 37°C in a 5% CO_2 incubator and split at 90% confluence. Cell culture media were exchanged with each fresh medium every 2 or 3 days.

2.3 | MTS assay

Cells were seeded (AsPC-1, 1×10^3 cells/well; BxPC-3, 1×10^3 cells/well; Capan-1, 1×10^3 cells/well; Capan-2, 1×10^3 cells/well; MIA PaCa-2, 1×10^3 cells/well; SW480, 1×10^3 cells/well; HCT 116, 1×10^3 cells/well; HT-29, 3×10^3 cells/well; COLO 205, 1×10^3 cells/well; MCF7, 1×10^3 cells/well; MDA-MB-231, 1×10^3 cells/well; BT-474, 1×10^3 cells/well; SKBR3, 1×10^3 cells/well; TOV-112D, 2×10^3 cells/well; SKOV3, 1×10^3 cells/well) into 96-well plates in 100 µL of complete medium and incubated for 24 h; then, treated with vehicle (DMSO) or 15, 30, or 60 µM of magnolin for 24, 48, or 72 h. To the cells in each well were added 20 µL of the MTS-based CellTiter 96®Aqueous One Solution. The mixture was incubated for 1 h at 37°C in a 5% CO_2 incubator and then absorbance at 492 nm was measured by using an xMark™ Microplate Absorbance Spectrophotometer (Bio-Rad Laboratories). Inhibition of cell proliferation by magnolin was evaluated by comparison with the absorbance of a vehicle-treated control group over 72 h at 24 h intervals.

2.4 | Anchorage-independent colony growth assay

Cells (8×10^3/well) suspended in 1 mL of top agar containing $1 \times$ BME supplemented with 10% FBS, 0.33% agar, and indicated doses of magnolin were plated onto 3 mL of solidified bottom agar containing $1 \times$ BME supplemented with 10% FBS, 0.5% agar, and indicated doses of magnolin and then cultured for 10–14 days at 37°C, in a 5% CO_2

incubator. Colony numbers were measured and scored by using an ECLIPSE Ti inverted microscope and the NIS-Elements AR (V.4.0) computer software program (NIKON Instruments Korea, Gangnam, Seoul, Korea).

2.5 | Cell-cycle analysis

TOV-112D (3×10^5) and SKOV3 (3×10^5) cells were seeded into 60-mm dishes and cultured overnight at 37°C in a 5% CO_2 incubator. Cells were treated with vehicle (DMSO) or 15, 30, or 60 µM of magnolin in complete medium for 12 h, then trypsinized, washed with ice-cold 1X PBS, and fixed with ice-cold 70% ethanol. The cells were treated with RNase A (200 µg/mL) and propidium iodide (20 µg/mL) for 15 min at 4°C. The cell-cycle phase distribution was determined by using flow cytometry (BD FACS Calibur™ flow cytometry, Franklin Lakes, NJ).

2.6 | Western blotting

To isolate the proteins for western-blot analysis, cells were disrupted by freezing and thawing in cell lysis buffer (50 mM Tris pH 8.0, 150 mM NaCl, 1% NP-40, Roche protease inhibitor cocktail [2.5 mM sodium pyrophosphate, 1 mM β-glycerophosphate, 1 mM sodium vanadate, and 1 mM phenyl methyl sulfonyl fluoride]), and the supernatant was recovered by centrifugation at 12 000 r/min for 5 min at 4°C. The protein concentration was determined by using the *DC* protein assay kit (Bio-Rad) and an equal amount of protein was resolved by performing SDS-PAGE. The proteins were transferred onto polyvinylidene fluoride (PVDF) membranes using transfer buffer (20 mM Tris-HCl [pH 8.0] containing 150 mM glycine and 20% [v/v] methanol), blocked with 5% nonfat dry milk in blocking buffer (1X TBS containing 0.05% Tween 20: [TBS-T]), and hybridized with antibodies against p-Akt, total-Akt, p-ERK1/2, total-ERK1/2, p-RSK, total-RSK, p-ATF1, total-ATF1, or β-actin overnight at 4°C. Blots were washed three times in 1X TBS-T buffer and rehybridized with appropriate HRP-conjugated secondary antibodies. Western blots were visualized with an enhanced chemiluminescence detection system (Amersham Biosciences, Piscataway, NJ, USA) using a ChemiDoc XRS imager system (Bio-Rad Laboratories).

2.7 | Senescence-associated β-galactosidase (SA-β-gal) assay

TOV-112D (2×10^4) and SKOV3 (1×10^4) cells were seeded into 24-well plate and cultured for 12 h. The cells were treated with the indicated doses of magnolin for 24 h, fixed with 4% formalin (250 µL per well) by incubation for 5 min at room temperature. Then, the cells were added 500 µL of SA-β-gal staining solution (40 mM citric acid/sodium phosphate [pH 6.0], 2 mM magnesium chloride, 150 mM NaCl, 5 mM potassium ferricyanide, 5 mM potassium ferrocyanide, 1% X-gal) and incubated at 37°C in an incubator for 12 h. The cells were observed, and the SA-β-gal-positive cells from computer-derived random images from four different areas were photographed and counted by using Adobe Photoshop (ver. 12.0).

2.8 | Semi-quantitative reverse transcription-polymerase chain reaction

Total RNA (2 µg) was reverse transcribed with N-MLV Reverse Transcriptase (iNtRON, Seongnam-si, Gyeonggi-do, Korea) and semi-quantitative PCR was performed with following primer pairs: *IL-6* forward 5′-TGG CTG AAA AAG ATG GAT GC-3′, reverse 5′-TGC AGG AAC TGG ATC AGG AC-3′; *IL-8* forward 5′-ATG ACT TCC AAG CTG GCC GTG GCT-3′, reverse 5′-TCT CAG CCC TCT TCA AAA ACT TCT C-3′; *IL-1b* forward 5′-TTT GAG TCT GCC CAG TTC CC-3′, reverse 5′-TCA GTT ATA TCC TGG CCG CC-3′; *MMP-1* forward 5′-CAT GAC TTT CCT GGA ATT GG-3′, reverse 5′-CCT GCA GTT GAA CCA GCT AT-3′; *MMP-3* forward 5′-ATG GAC AAA GGA TAC AAC AGG GA-3′, reverse 5′-TGT GAG TGA GTG ATA GAG TGG G-3′; *β-actin* forward 5′-CGT CTT CCC CTC CAT CG-3′, reverse 5′-CTC CTT AAT GTC ACG CAC-3′. PCR products were visualized by agarose gel electrophoresis and ethidium bromide staining.

2.9 | NF-κB reporter gene assay

TOV-112D (1.5×10^5) and SKOV3 (7×10^4) cells were seeded into 12-well plate and cultured overnight. The cell were co-transfected with *NF-κB* luciferase reporter plasmid (0.5 µg) and *pRL-SV40 Renilla* luciferase reporter plasmid (20 pg) and cultured for 24 h. The cell were starved in serum-free medium for 16 h, pretreated with magnolin with indicated doses for 30 min and then co-treated EGF (10 ng/mL) and magnolin for 24 h. The cells were disrupted, and the firefly luciferase activity was measured using a VIXTOR X3 (PerkinElmer Inc, Waltham, MA). The firefly luciferase activity was normalized by *Renilla* luciferase activity to equalize the transfection efficiency.

2.10 | Cancer stem cell analysis

Cells (TOV-112D, $6 \times 10^3/20$ µL; SKOV3, $6 \times 10^3/20$ µL) were seeded as 20 µL drops onto the lids of 100-mm culture dishes by using hanging drop method[14] and then cultured for 48 h at 37°C in a 5% CO_2 incubator. Cells were dissociated by using accutase (Sigma-Aldrich), harvested, and hybridized with CD44 (4 ng/µL) or CD24 (2 ng/µL) in the dark for 2 h at 4°C. The cells were counted by flow cytometry (BD FACS Calibur™ flow cytometer).

2.11 | Xenograft athymic animal experiment

Athymic nude mice (6 weeks old) were obtained from Charles River (Seoul, South Korea) and maintained under specific pathogen-free conditions with a light/dark cycle of 12/12 h in accordance with the guideline approved by the Institutional Animal Care and Use Committee (approval number: 2014-013-02) at The Catholic University of Korea. After 1 week of acclimation, the mice were implanted subcutaneously with TOV-112D (6×10^6 cells) in the right dorsal flank and monitored until tumor volume had grown to 100 mm³. Mice harboring a tumor larger than 100 mm³ were randomly divided into two groups for vehicle treatment (control group: $n = 12$) or 100 mg/kg

of Shin-Yi fraction one treatment ($n = 13$). Treatments were administered by orally every day for 12 days and tumor growth was measured twice a week. Tumor volume was calculated from measurements of diameters of the individual tumor by using the following formula: tumor volume (mm³) = (length × width × height × 0.52). Treated mice were monitored until tumors reached 1 cm³ total volume, at which time mice were euthanatized and tumors extracted.

2.12 | Immunohistofluorescence assay

To confirm the expression of p16^Ink4a and p27^Kip1 in xenograft tumor tissues, the paraffin-invaded tumor tissue slide was deparaffinized by incubation at 60°C for 2 h, rehydrated and unmasked by boiling with 10 mM sodium citrate buffer (pH 6.0) for 10 min. After cooling, the slide was blocked with 5% goat serum in 0.5% Triton X-100/PBS at RT for 1 h and hybridized with the indicated antibodies against p16^Ink4a (200:1) and p27^Kip1 (200:1) at 4°C overnight. The slide was three times washed and hybridized with secondary antibodies conjugating Alexa-568 at RT for 2 h. Images were captured using laser scanning confocal microscope (LSM 710) and the intensity was analyzed by Image J computer software program (Ver. 1.6).

2.13 | Statistical analysis

Data are presented as the mean ± SEM. The Student's *t*-test was used to perform statistical analysis of single comparisons. A probability value of $P < 0.05$ was used as the criterion for statistical significance.

3 | RESULTS

3.1 | Magnolin suppresses cell proliferation of TOV-112D cells among tested pancreatic, colon, breast, and ovarian cancer cells

Recently, our research group demonstrated that magnolin, a natural compound abundantly found in Shin-Yi, inhibits cell proliferation and transformation induced by tumor promoters such as EGF in JB6 Cl41 cells.[13] Molecular targeting against kinases demonstrated that magnolin targets the active pockets of ERK1 and ERK2, which are important kinases transducing the activation signaling of EGFR/Ras/Raf/MEKs to RSK and/or transcription factors that are highly activated in many solid human cancers,[15] at approximately 87 and 16 nM of IC_{50}, respectively.[13] However, the anticancer activity of magnolin has not been clearly elucidated. To explore the anticancer activity of magnolin, we utilized several cancer cells including pancreatic cancer cells (AsPC-1, BxPC-3, Capan-1, Capan-2, and MIA PaCa-2), colon cancer cells (SW480, HCT 116, HT-29, and COLO 205), breast cancer cells (MCF7, MDA-MB-231, SKBR3, and BT-474), and ovarian cancer cells (TOV-112D and SKOV3). Since it has been reported that cancer cells originating from different organs or tissues harbor predominantly different mutation(s) in different genes,[15,16] we firstly analyzed mutations of oncogenes and tumor suppressor genes against the aforementioned cancer cell lines by searching the CCLE

(https://portals.broadinstitute.org/ccle_legacy/home) mutaome database (Table 1). The results showed that pancreatic cancer cells exhibited gain-of-function mutations, mainly in MAPK, and loss-of-function mutations, mainly in p16, p53, and SMAD4 (Table 1). The colon cancer (COLO 205, HT-29, SW480, and HCT 116) and breast cancer (MCF7, BT-474, MDA-MB-231, and SKBR3) cell lines showed variable gain-of-function mutations in both PI3 K and MAPK or Wnt and MAPK signaling pathways, respectively (Table 1). Interestingly, the majority of these cell lines harbored gain-of-function mutations in double or triple signaling pathways and single tumor suppressor signaling pathways such as p16 or p53 (Table 1). Furthermore, TOV-112D ovarian cancer cells had a mutation in β-catenin but not in Ras or PI3 K. In contrast, SKOV3 ovarian cancer cells had a constitutively active mutation of PI3 K together with loss-of-function mutations of the p16 and p53 tumor suppressors (Table 1). In addition, we analyzed the magnolin effects on cell proliferation in pancreatic, colon, breast, and ovarian cancer cell lines. Since pancreatic cancer cells harbored mainly gain-of-function mutation in K-Ras and MAP2K4 and loss-of-function mutation in p16 and p53 (Table 1), we expected that inhibition of ERK1 and ERK2 might sensitize pancreatic cancer cell proliferation to directly inhibit cell proliferation. Unexpectedly, pancreatic cancer cell proliferation was not affected by magnolin treatment (Figure 1A). Moreover, the SW480 and HCT116 colon cancer cells and the MCF-7, MDA-MB-231, and SKBR3 breast cancer cells showed about 20–30% cell proliferation inhibition at the 60 μM magnolin treatment concentration along with dose-dependency; regardless, magnolin did not have significant inhibitory effect on proliferation in these cell lines (Figure 1B and C). An interesting result was obtained from the ovarian cancer cells TOV-112D (harboring gain-of-function mutation in β-catenin) and SKOV3 (harboring gain-of-function mutation in PI3 K and loss-of-function mutation in p15 and p53 tumor suppressors) with only TOV-112D ovarian cancer cells showing an inhibitory effect of magnolin on cell proliferation, and that effect was dose-dependent (Figure 1D). These results indicate that investigations of chemotherapeutic applications that target ERK1 and ERK2 can benefit to treat cancer cells with non-mutated tumor suppressor linkage.

3.2 | Magnolin inhibits cell-cycle transition and colony growth in TOV-112D, but not in SKOV3

The Ras/Raf/MEKs/ERKs/RSK2 signaling pathway has an important role in cell proliferation and cancer development by stimulation of growth factors.[17] Our previous results demonstrated that inhibition of ERK1 and ERK2 by magnolin suppresses G1/S cell-cycle transition in premalignant JB6 Cl41 cells.[13] Therefore, based on the results presented in Figure 1 and Table 1, we hypothesized that magnolin might differentially inhibit cell-cycle arrest in TOV-112D and SKOV3 ovarian cancer cells. To examine that hypothesis, we initially conducted cell-cycle analysis under normal cell culture conditions. We observed that magnolin treatment increased the populations of G1 and G2/M phase cells in TOV-112D ovarian cancer cells in a dose-dependent manner (Figure 2A, left graph). In contrast, the population

TABLE 1 CCLE mutaome analysis of genes involved in chemoresistance

Cancer type	Cell line	PI3KCA	CTNNB1	APC	KRAS	BRAF	MAP2K4	EGFR	CDKN2A	TP53	BRCA2	RB1	PTEN	SMAD4	NOTCH1	MLH1	SMO	NF1	UTX	SMARCA4	CDH1	FBXW7	NF2	STK11
Pancreatic cancer	MIA PaCa-2				O				X	X				X					X					
	AsPC-1				O		O		X	X				X								X		
	Capan-1				O		O		X	X	X			X										
	Capan-2				O				X															
	BxPC-3							O	X	X				X										
Colon cancer	COLO 205		O	X			O			X				X										
	HT-29	O		X	O	O				X				X										
	SW480			X	O																			
	HCT116	O	O		O					X				X	△	X	X			X	X			
Breast cancer	MCF7	O		X					X															
	BT-474	O					O																	
	MDA-MB-231				O	O			X	X													X	
	SK-BR-3																			X				
Ovarian cancer	TOV-112D		O																					
	SKOV3	O							X	X												X		

O, gain-of-function; X, loss-of-function; △, not determined.
Summary of Cancer Cell Line Encyclopedia (CCLE) mutation data for gain/loss-of-function mutations in human cancer cell lines.
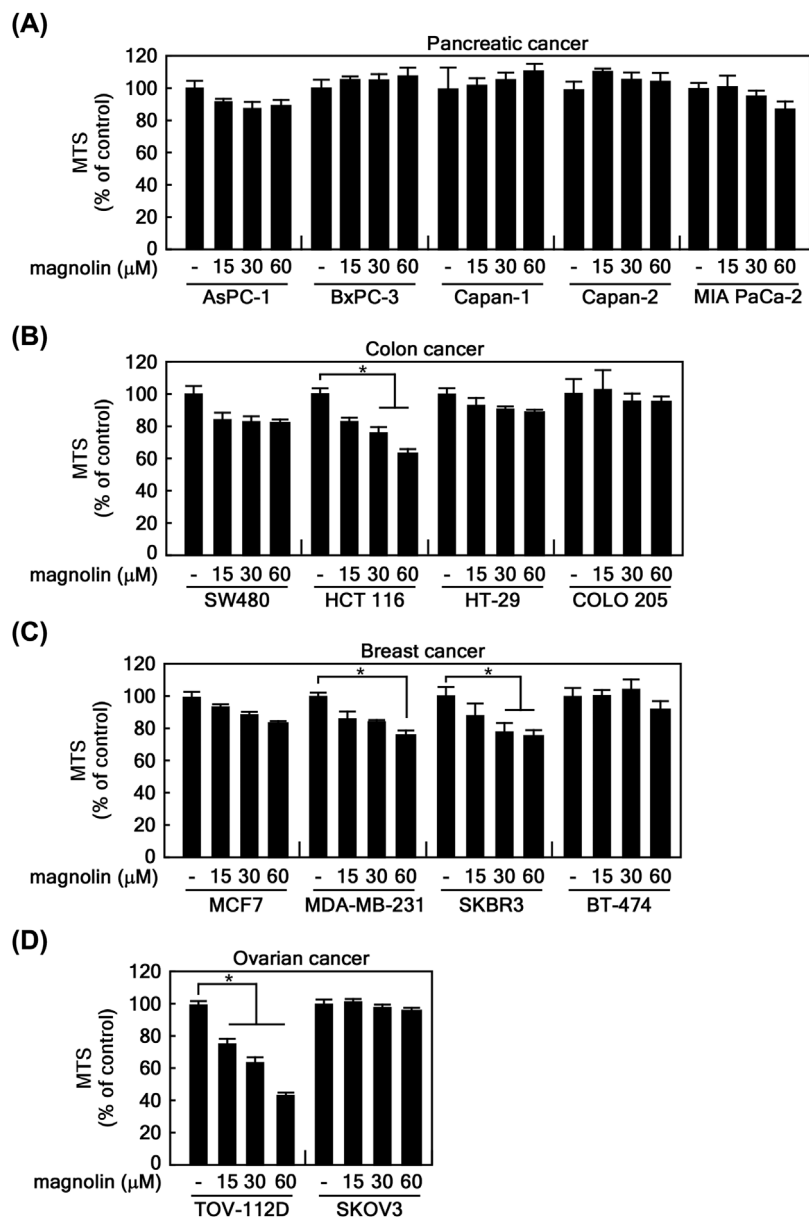
FIGURE 1 Screening of cancer cell lines showing results for sensitivity against magnolin. (A) Pancreatic cancer cells (AsPC-1, 1×10^3 cells/well; BxPC-3, 1×10^3 cells/well; Capan-1, 1×10^3 cells/well; Capan-2, 1×10^3 cells/well; MIA PaCa-2, 1×10^3 cells/well), (B) colon cancer cells (SW480, 1×10^3 cells/well; HCT 116, 1×10^3 cells/well; HT-29, 3×10^3 cells/well; COLO 205, 1×10^3 cells/well), (C) breast cancer cells (MCF7, 1×10^3 cells/well; MDA-MB-231, 1×10^3 cells/well; BT-474, 1×10^3 cells/well; SKBR3, 1×10^3 cells/well), and (D) ovarian cancer cells (TOV-112D, 2×10^3 cells/well; SKOV3, 1×10^3 cells/well) were seeded into 96-well cell culture plates and cell proliferation was measured at 24 h intervals over 96 h by performing MTS assays. The graphs denote inhibition percentage of cell proliferation at 72 h compared to non-magnolin-treated control cells. (A–D) Data were obtained from three independent experiments, values are presented are means ± SEM. Biological significance was determined by comparison with the non-magnolin-treated control group and statistical significance values (*$P < 0.01$) were calculated by Student's t-test

of S phase cells decreased under magnolin treatment in a dose-dependent manner (Figure 2A, left graph). However, no significant changes of cell cycle phases were observed in SKOV3 cells at 60 µM of magnolin (Figure 2A, right graph). These results further suggested that magnolin may inhibit TOV-112D colony growth, but not that of SKOV3, under anchorage-independent conditions. To confirm that hypothesis, we conducted soft agar assays. We observed that magnolin inhibited colony growth of TOV-112D cells by approximately

50% at 30 µM in soft agar (Figure 2B, upper panels and graph), and the inhibitory effect of magnolin on colony growth in soft agar increased in a dose-dependent manner (Figure 2B, upper panels and graph). In contrast, SKOV3 cells did not alter the colony growth by magnolin treatment in soft agar (Figure 2B, bottom panels and graph). Taken together with Table 1 and Figures 1 and 2, these results demonstrate that magnolin treatment may be useful for inhibiting the growth of cancer cells harboring gain-of-function mutation in the Wnt signaling
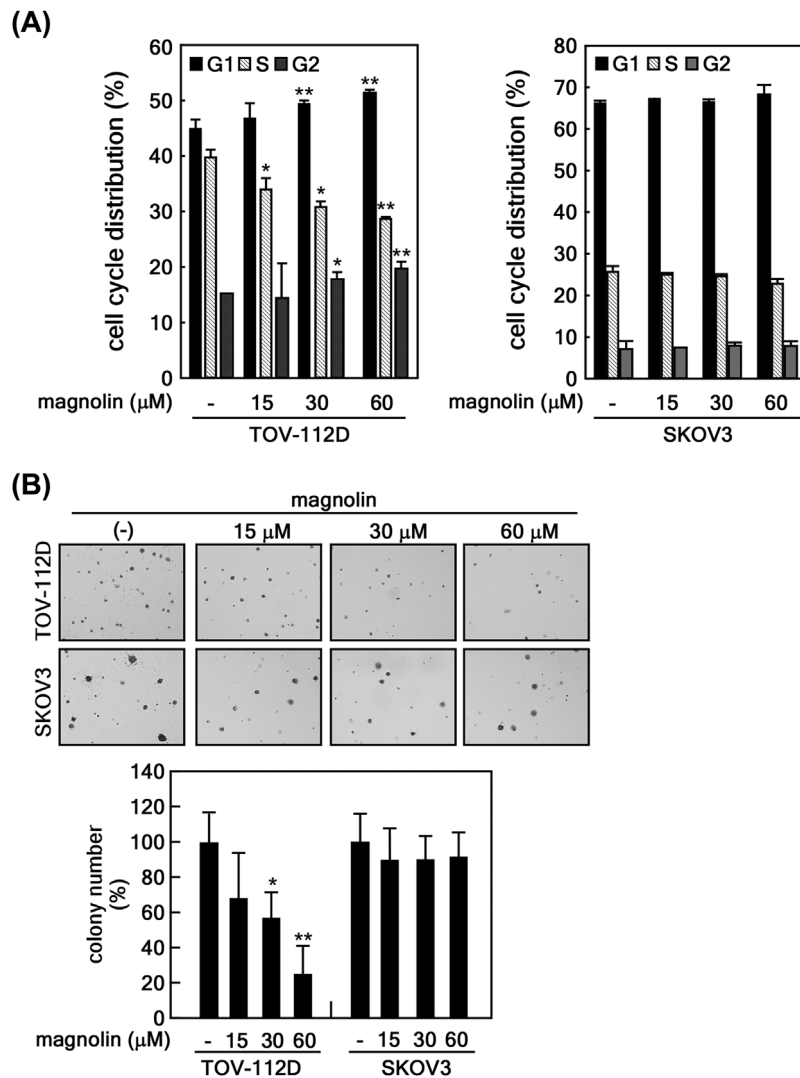
(A)

(B)

FIGURE 2 Magnolin sensitivities of TOV-112D and SKOV3 ovarian cancer cells on cell proliferation and colony growth. (A) Magnolin inhibited cell proliferation of TOV-112D cells, but not SKOV3 cells. TOV-112D (8×10^5 cells) and SKOV3 (4×10^5 cells) cells were seeded into 60-mm dishes and cultured overnight. The cells were treated with indicated doses of magnolin for 12 h, and then cell-cycle cell phase distribution was analyzed by using flow cytometer as described in Materials and Methods. (B) Magnolin suppressed anchorage-independent colony growth of TOV-112D cells, but not SKOV3 cells. TOV-112D or SKOV3 cells (8×10^3 cells) suspended in BME medium containing 0.3% agar supplemented with 10% FBS and vehicle (DMSO) or 15, 30, or 60 μM of magnolin. Cultures were maintained at 37°C in a 5% CO_2 incubator for 20 days, and the colonies were counted under an ECLIPSE Ti inverted microscope using the NIS-Elements AR (V. 4.0) computer software program. (A and B) Data were obtained from three independent experiments, values presented are means ± SEM. Biological significance was determined by comparison with the non-magnolin-treated control group and statistical significance values (*$P < 0.05$, **$P < 0.01$) were obtained by Student's t-test

pathway, such as the β-catenin mutation in ovarian cancer. The results also suggest that ovarian cancer cells harboring a constitutively active mutation of PI3 K and loss-of-function mutations of p16 and p53 tumor suppressor proteins can show chemoresistance to ERK1 and ERK2 inhibitors.

3.3 | Magnolin sensitivity associated with ERK1/2 phosphorylation levels in ovarian cancer cells

To examine the signaling pathways related to the sensitivities of magnolin on cell proliferation and colony growth in soft agar, we analyzed the phospho-protein profiles of ERKs and RSKs as members

of MAPK, Akt as a member of PI3 K, and ATF1 as a member of RSK2 downstream targets in cancer cell lines such as Capan-1, MIA PaCa-2, MDA-MB-231, MCF7, HCT116, HT-29, TOV-112D, and SKOV3 (Figure 3A). We observed that the phosphorylation levels of ERK1/2 were higher in ovarian cancer cells than in other cancer cells (Figure 3A, lane 7 and 8). Interestingly, the phospho-RSK level at Thr359/363, an amino acid directly phosphorylated by ERK1/2, was higher in MDA-MB-231, HCT116, and HT-29 cells, whereas these cells contained relatively low levels of phospho-ERK1/2 (Figure 3A, lane 3, 5, and 6) compared to the ovarian cancer cells (Figure 3A, lane 7 and 8). Moreover, the phosphorylations of Akt at Thr308, an amino acid directly phosphorylated by PI3 K and PDK1, and Ser473, a target
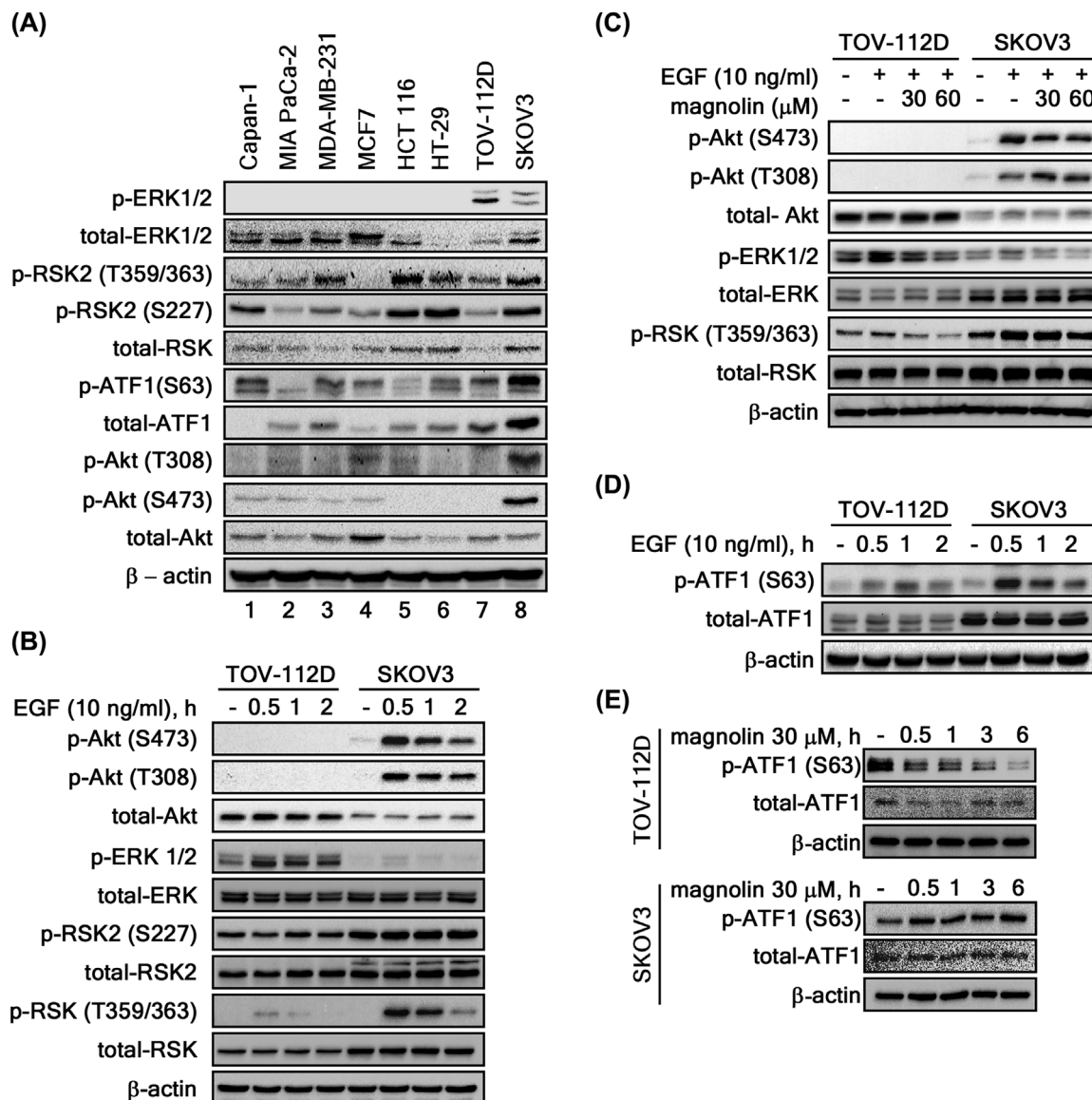
(A)

(B)

(C)

(D)

(E)

FIGURE 3 Comparison of the phospho-protein profiles in two ovarian cancer cell lines. (A) Phospho-protein profiles in cancer cells. Indicated cancer cells (1×10^6 cells) were seeded into 100-mm cell culture dishes and cultured until cell confluence of approximately 90%. The proteins extracted from indicated cells were visualized by western blotting using specific antibodies as indicated. (B) Activation protein profiles following EGF stimulation of ovarian cancer cells. TOV-112D (2×10^6 cells) and SKOV3 (1×10^6 cells) cells were seeded into 100-mm cell culture dishes, cultured for 24 h, and starved with non-FBS containing medium for 18 h. Cells were stimulated with EGF (10 ng/mL) for the indicated time course. The proteins were extracted and visualized by western blotting using specific antibodies as indicated. (C) Inhibitory phospho-protein profiles by co-treatment of EGF and magnolin in ovarian cancer cells. TOV-112D (2×10^6 cells) and SKOV3 cells (1×10^6 cells) were seeded into 100-mm cell culture dishes, cultured for 24 h, and starved with non-FBS containing media for 18 h. The cells were pretreated with the indicated dose of magnolin for 30 min and then co-treated with EGF (10 ng/mL) for 30 min. The proteins were extracted and visualized by western blotting using specific antibodies as indicated. (D) Comparison of phospho-ATF1 protein levels in ovarian cancer cells. TOV-112D (2×10^6 cells) and SKOV3 (1×10^6 cells) cells were seeded into 100-mm cell culture dishes, cultured for 24 h, and starved with non-FBS containing medium for 18 h. The cells were stimulated with EGF (10 ng/mL) for the indicated time course. The proteins were extracted and phospho-ATF1 and total-ATF1 were visualized by western blotting using specific antibodies as indicated. (E) Magnolin inhibited the phosphorylation of ATF1 in TOV-112D cells, but not in SKOV3 cells. TOV-112D (2×10^6 cells) and SKOV3 (1×10^6 cells) cells were seeded into 100-mm cell culture dishes, cultured for 24 h, and treated with 30 μM of magnolin for the indicated time course. The proteins were extracted and phospho-ATF1 and total-ATF1 were visualized by western blotting using specific antibodies as indicated. (A–E) β-actin was used for the internal control to verify equal protein loading
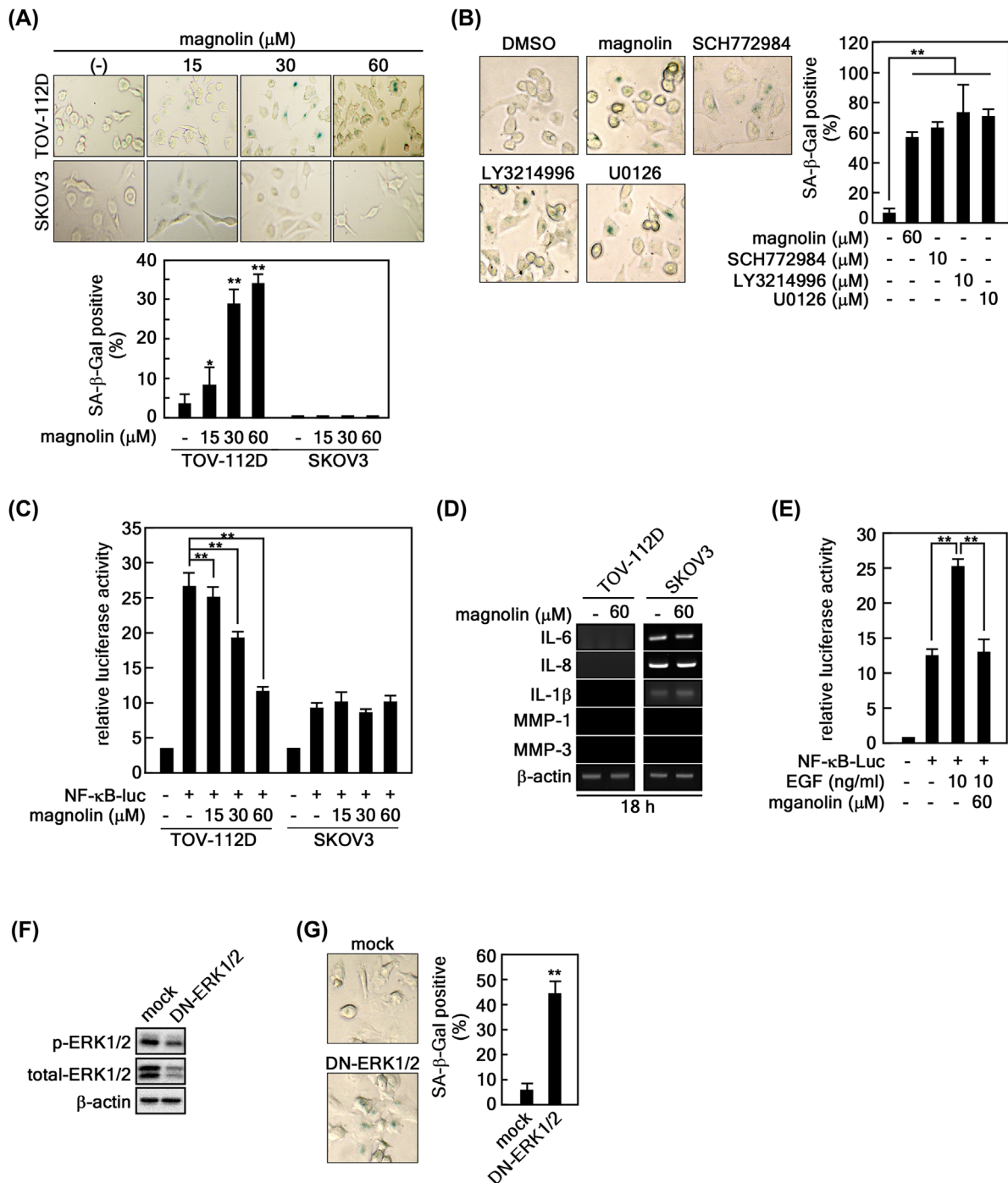
(A)

(B)

(C)

(D)

(E)

(F)

(G)

FIGURE 4 Continued.

amino acid phosphorylated by mTOR complex 2 (mTORC2), were strongly observed in SKOV3 cells compared to the other cancer cells (Figure 3A, lane 8 vs. lane 1–7). Since ovarian cancer cells showed a marked difference in phospho-ERK1/2 and phospho-Akt levels, we further examined the EGF-stimulated responsiveness of phospho-protein profiles under complete medium-supplemented normal cell culture conditions (Figure 3B). The results indicated that phospho-ERK1/2 and phospho-RSK levels were induced by EGF stimulation in TOV-112D cells (Figure 3B). Interestingly, SKOV3 cells showed only a marginal increase in ERK1/2 phosphorylation following EGF

stimulation (Figure 3B). However, phospho-RSK at Thr359/Ser363, phospho-RSK2 at S227, and total protein levels of RSKs were higher in SKOV3 cells than in TOV-112D cells (Figure 3B). To examine the effects of magnolin on the phosphorylation levels in signaling pathways, we co-stimulated TOV-112D and SKOV3 cells with EGF and magnolin. We found that magnolin suppressed the EGF-induced RSK phosphorylation at Thr359/Ser363 in a dose-dependent manner as similar as a decrease of ERK1/2 phosphorylation (Figure 3C). Interestingly, although phosphorylation of ERK1/2 was very weakly increased by EGF stimulation in SKOV3 cells, the phosphorylation

levels of RSKs at Thr359/Ser363 were also markedly increased by EGF stimulation in SKOV3 cells (Figure 3C). Additionally, magnolin minimally reduced the EGF-induced phospho-RSK levels in SKOV3 cells compared to that in TOV-112D cells (Figure 3C). Although the increased ratio for phosphorylation of ATF1 at Ser63, which is a target amino acid phosphorylated by RSK2,[18] was similarly increased in both TOV-112D and SKOV3 cells, the SKOV3 cells showed a more marked increase in phopsho-ATF1 levels because of high degree of elevated ATF1 protein levels in SKOV3 cells (Figure 3D). Moreover, we confirmed that magnolin suppressed ATF1 phosphorylation only in TOV-112D cells, not in SKOV3 cells, under normal cell culture conditions (Figure 3E). Taken together with the results in our previous study,[13] these results demonstrate that molecular targeting of ERK1 and ERK2 with magnolin can suppress ovarian cancer cell lines harboring a general MAPK signaling cascade such as TOV-112D. These results also suggest that cells containing a bypass signaling pathway of ERK1/2 may induce chemoresistance against therapeutic compounds that target RSK upstream signaling molecules in Ras/Raf/ MEKs/ERKs signaling axis.

3.4 | Magnolin induces cellular senescence in TOV-112D, but not in SKOV3

The suppression of cancer cell proliferation induces cellular senescence.[19] Our results demonstrated that magnolin treatment in TOV-112D ovarian cancer cells inhibits cell proliferation by enhancing accumulation of cells at the G1 cell-cycle phase (Figures 1D and 2A). Moreover, Ras activation induces the Raf/MEKs/ERKs/RSK2 signaling axis, resulting in increase of cancer cell proliferation.[20] Taken together, these observations suggest that inhibition of cell proliferation by magnolin might induce cellular senescence in TOV-112D cells. To examine that hypothesis, we conducted senescence associated (SA)-β-gal assays using TOV-112D and SKOV3 cells (Figure 4A). We observed

that magnolin treatment increased SA-β-gal-positive cell population in TOV-112D cells in a dose-dependent manner (Figure 4A). In contrast, we did not observed SA-β-gal-positive SKOV3 cells while the magnolin concentration was increased to 60 μM (Figure 4A). The SA-β-gal-positive staining of TOV-112D cells was not limited by magnolin, but observed in other ERK inhibitors such as SCH772984 and LY321449 and a MEK inhibitor U0126 (Figure 4B). As expected, TOV-112D cells was showed the SA-β-gal-positive cells by specific inhibition of ERKs using SCH772984, but not in SKOV3 (Supplementary Figure S1). To examine whether magnolin-induced senescence is the cellular senescence or senescence-associated secretory phenotype (SASP), we firstly examine the transactivation activity of NF-κB, which is an important transcription factor inducing gene expression of SASP related genes.[21] Our results demonstrated that magnolin suppressed NF-κB transactivation activity (Figure 4C) as similar as our previous report.[22] In contrast, the inhibition of NF-κB transactivation activity was not observed in SKOV3 cells (Figure 4C). Moreover, magnolin did not induce or not alter the expression of IL-6, IL-8, IL-1β, MMP-1, and MMP-3 (Figure 4D), which are well known the representative SASP markers.[23] Notably, NF-κB transactivation activity induced by EGF stimulation was suppressed by magnolin treatment (Figure 4E). Importantly, suppressed ERK phosphorylation by transfection of dominant negative of ERK1/2 (Figure 4F) induced SA-β-gal-positive cell population (Figure 4G). Taken together, inhibition of ERK1/2 by magnolin induces cellular senescence, not SASP, in TOV-112D, resulted in inhibition of TOV-112D proliferation.

3.5 | Magnolin suppresses cancer growth of TOV-112D in vivo

A recent study demonstrated that cancer cells harboring cancer stem cell properties resist cellular senescence.[24] To examine whether SKOV3 cells harbor cancer stem cell properties, we undertook sphere

FIGURE 4 Magnolin suppresses TOV-112D ovarian cancer growth, but not SKOV3 growth, in xenograft athymic nude mice by inducing cellular senescence. (A) Magnolin induced SA-β-gal staining in TOV-112D cells, but not in SKOV3 cells. TOV-112D (2×10^4) and SKOV3 (1×10^4) cells were seeded into 24-well plates, cultured, and treated with indicated doses of magnolin for 24 h. (B) ERK inhibition induces SA-β-gal staining. TOV-112D (2×10^4) cells were seeded into 24-well plates, cultured, and treated with indicated doses of magnolin, SCH772984, LY3214996 and U0126 for 24 h. (C) Magnolin suppresses NF-κB transactivation activity. NF-κB-luciferase reporter plasmids were transiently transfected into TOV-112D and SKOV3 cells and cultured for overnight. The cells were treated with indicated doses of magnolin for 12 h and firefly luciferase activities were measured. The equal transfection of NF-κB-luc was compensated using pRL-SV40 Renilla luciferase control plasmids. (D) Magnolin did not alter the gene expression of SASP makers. Total RNA extracted from the magnolin treated TOV-112D and SKOV3 were utilized to measure the gene expression of SASP maker genes by PCR as indicated. The PCR products were visualized by ethidium bromide containing agarose-gel electrophoresis under UV lamp. β-actin was used for the internal control to verify equal experimental condition. (E) Magnolin inhibits EGF-induced NF-κB transactivation activity. NF-κB luciferase reporter plasmids were transfected into TOV-112D cells, starved and treated with EGF or EGF/magnolin for 12 h and firefly luciferase activity was measured. The equal transfection of NF-κB-luc was compensated using pRL-SV40 Renilla luciferase control plasmids. (F) Dominant negative (DN)-ERK suppresses ERK phosphorylation. The expression vector encoding DN-ERK was transfected into TOV-112D and confirmed the suppression of ERK phosphorylation by Western blotting. β-actin was used for the internal control to verify equal protein loading. (G) DN-ERK induces SA-b-gal staining. The pDN-ERK expression vector was transfected into TOV-112D cells and cultured 24 h. The cells were stained with X-gal and observed under a light microscope (X400). (A, B, and G) The cells were fixed, and cellular senescence was observed under a light microscope after SA-β-gal staining. The SA-β-gal-positive cells from computer-derived random images from four different areas were measured and the relative abundance (%) of SA-β-gal-positive cells are presented in lower graph. (A–C, E, and G) Data were obtained from three independent experiments, values presented are means ± SEM. Biological significance was determined by comparison with the non-magnolin-treated or indicated control group and statistical significance values (*$P < 0.05$, **$P < 0.01$) were determined by Student's t-test

colony formation of TOV-112D and SKOV3 cells. Using sphere-formed colonies, we examined the cell populations expressing cancer stem cell markers via flow cytometry using CD24 and C44 antibodies. The results demonstrated that SKOV3 cells produced increased CD44$^+$/CD24$^-$ cell populations, which is a typical cancer stem cell marker of ovarian cancer stem cells.[25,26] In contrast, the CD44$^+$/CD24$^-$ cell population in TOV-112D cells did not significantly change after sphere formation (Figure 5A). Taken together with Figures 2B and

4A and B, we hypothesized that magnolin might suppress TOV-112D cancer cell growth in athymic nude mice. Unfortunately, there was difficulty obtaining a sufficient quantity of magnolin with a purity level of at least 97% or higher. Thus, we utilized a half purified Shin-Yi fraction 1 in which magnolin was approximately 53% of the total fraction. We implanted TOV-112D cells (6×10^6 cells) in the right dorsal flank of athymic nude mice, and when tumor growth reached approximately 100 mm^3, we randomly divided the mice into two
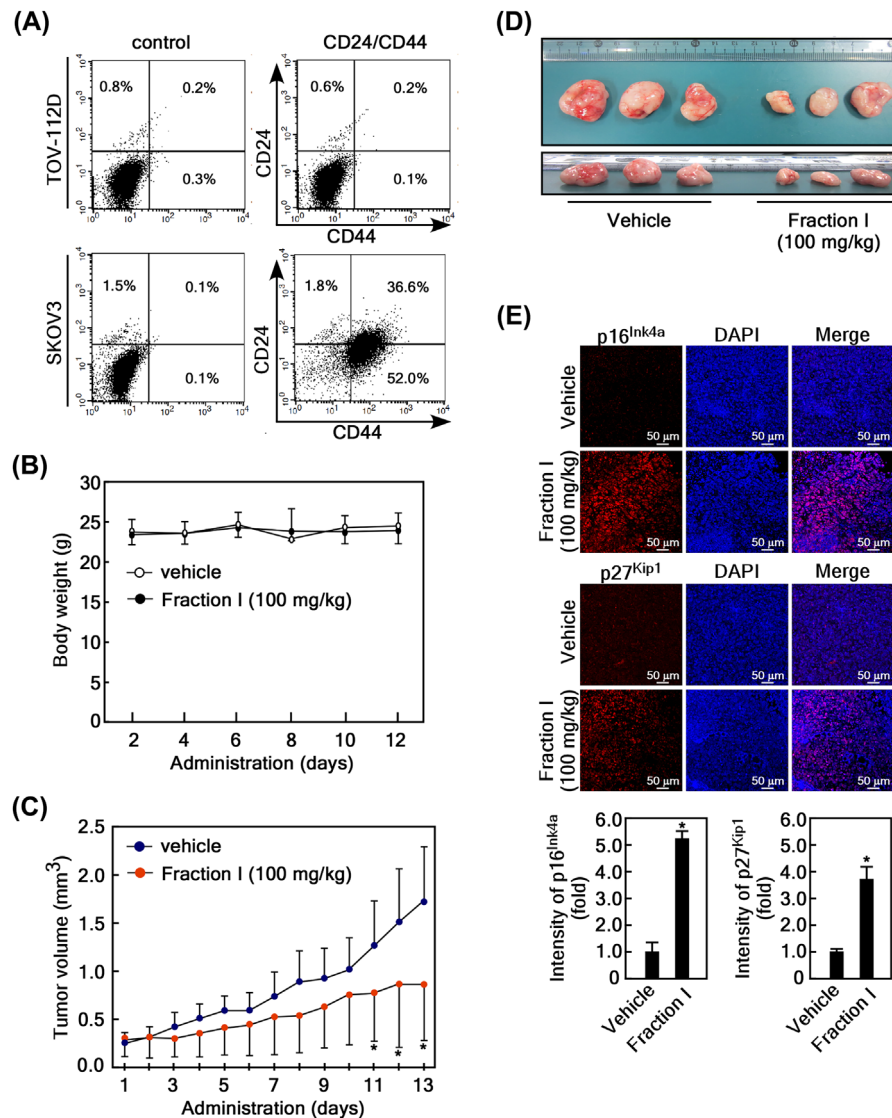

FIGURE 5 Magnolin induces cellular senescence in vivo. (A) SKOV3 cells harbor ovarian cancer stem cell properties. TOV-112D (6×10^3/20 μL) and SKOV3 (6×10^3/20 μL) cells were applied to form mono spheres (100 spheres) by using hanging drop culture for 48 h. The cells were detached with accutase and hybridized with CD24-APC- or CD44-FITC-conjugated antibodies for 2 h on ice, and the CD24- and CD44-positive/negative populations were analyzed by flow cytometry. (B-D) Magnolin suppressed TOV-112D cancer growth in the xenograft animal model. Athymic nude mice maintained under specific pathogen-free conditions and a light/dark cycle of 12/12 h underwent subcutaneous implantation of TOV-112D cells (6×10^6 cells) in the right dorsal flank in accordance with the approved animal care guideline as described in Materials and Methods. When tumors had grown to over 100 mm^3, mice were divided into two groups and orally administrated vehicle (control group: $n = 12$) or Shin-Yi fraction 1 magnolin extract (100 mg/kg, $n = 13$) for 12 days every day. Body weight (B) and tumor growth (C, $^*P < 0.05$) were measured twice a week. At the end of the treatment period, the mice were euthanatized and tumors were excised (D). (E) The tumor tissues obtained from vehicle and fraction I administered experimental group were prepared tissue slides for histological analysis. The tissue slides were processes for immunohistofluorescence analysis as described in "Materials and Methods." The protein levels of p16^{Ink4a} and p27^{Kip1} were visualized by hybridization using specific primary and Alexa-568. Fluorescence images were detected and captured under confocal microscope. DAPI was used for nuclei staining

groups and orally administered vehicle or 100 mg/kg of Shin-Yi fraction 1 every day for 12 days. The administration of fraction I did not affect mouse body weight change during the treatment period (Figure 5B), indicating that Shin-Yi fraction 1 had no apparent toxicity. However, the results showed that Shin-Yi fraction 1 significantly suppressed growth of TOV-112D tumors in athymic nude mice (Figure 5C and D). Since magnolin induced cellular senescence (Figure 4), we further analyzed protein levels of p16[Ink4a] and p27[Kip1], which were typical cellular senescence markers, in xenograft tumor tissues. We found that tumor tissues from fraction I administered mice showed higher p16[Ink4a] and p27[Kip1] protein levels than that of vehicle administered mice (Figure 5E). Taken together, these results demonstrate that magnolin may have application as a cancer therapeutic agent against ovarian cancer cells that do not have a gain-of-function mutation in PI3 K and a loss-of-function mutation in p16 and p53 tumor suppressor proteins.

4 | DISCUSSION

Chemoresistance of cancer cells is principally obtained via two different pathways, intrinsic and extrinsic, and such resistance can affect cancer cell survival and stress tolerance.[27] The intrinsic pathway has an important role in drug metabolism in the liver by activating phase I, phase II, and phase III drug metabolizing enzymes.[28] The extrinsic pathway is involved in genetic and epigenetic chemo-resistance alterations, resulting in alteration of gene expressions.[27] Generally, genetic alteration of tumor suppressor proteins such as p16, p21, and p53 has a key role in the chemoresistance of various cancer cells.[29] However, signaling studies focused on a specific signaling pathway have not fully elucidated the complicated signaling networks involved in responses to diverse intrinsic and extrinsic stimuli.[30] To assist in that elucidation, the National Cancer and National Human Genome Research Institutes have provided mutaome data obtained from various cancer cells.[31] Those data can provide important clues in researching the relationship between genetic alteration and chemoresistance.

One of the widely reported ways to obtain cancer chemo-resistance is to alter the molecular targets of therapeutic agents by modulating gene expression levels or bypassing the target signaling pathway.[32,33] Although MAPK and PI3 K/Akt signaling pathways are involved in cancer development and chemoresistance, they are generally recognized as two independent but parallel pathways.[33] However, recent interactome studies have indicated that these two signaling pathways influence each other in different signaling transduction processes, both negatively and positively, via multiple cross-talking points.[34] In this study, we observed that ERK1/2 phosphorylation resulting from EGF stimulation in SKOV3 cells was notably weak compared to that in TOV-112D cells (Figure 3B). Interestingly, SKOV3 cells contained high levels of Akt phosphoryla-tion at Thr308 and Ser473, which are critically important to full activation of Akt. Importantly, SKOV3 cells showed very strong responsiveness for RSK phosphorylation at Thr359 and Thr363

(Figure 3B), which are critically important for RSK activation.[20] The results showing that SKOV3 cells exhibited magnolin resistance during cell proliferation and colony growth in soft agar (Figure 1D and 2B) suggest that there may be another contact point, one that does not involve ERK1 or ERK2.

Cancer cells harbor the ability to sustain chronic proliferation. In contrast, normal tissues exhibit controlled production and release of growth-promoting signals, ensuring homeostasis of cell numbers for the maintenance of normal tissue function.[35] Thus, elucidation of the mechanisms regulating cell proliferation in normal cells and tissues is important because cancer cells acquire the capability to sustain proliferation via various alternative signaling pathways.[36] Cancer cells may produce auto-growth factor themselves, resulting in autocrine proliferative stimulation.[37] Moreover, loss of regulatory mechanisms controlling cell proliferation can also result from mutation.[38] For example, human melanomas contain about 40% of the activating mutations in B-Raf, resulting in constitutive activation signaling through the Raf to MAPK pathways.[39] Similarly, mutation in the catalytic subunit of PI3 K has been reported in several different human cancers,[40] and the signaling pathway through PI3 K to Akt/mTOR kinase has been reported to coordinate and sustain cancer cell proliferation, growth, and division via regulation of cellular metabolism and homeostasis.[41] Recently, oncogenes such as K-Ras have been shown to mediate cellular and metabolic transformation during tumorigenesis,[42] indicating that MAPK and PI3 K signaling pathways are related to the maintenance of homeostasis in normal and cancer cells.[43] One path to the induction of cancer chemoresistance is the bypassing of cellular senescence, a self-protection mechanism,[44] resulting in immortalization and malignancy. An accumulation of data has indicated that the loss-of-function of tumor suppressors, such as retinoblastoma (RB), p53, and p16, has a critically important role in the process of bypassing cellular senescence.[45,46] Moreover, the loss of p53 and the tumor suppressor PTEN bypasses cellular senescence to form prostate cancer in mice.[46] Interestingly, mutations in the Ras-mediated MAPK family, especially the B-Raf valine-to-glutamate mutation, encourage enhancement of tumorigenesis in melanoma by evasion of p53-dependent senescence.[47] Our current study demon-strated that TOV-112D harbors wildtype p16 and p53 and SKOV3 contains mutant p16 and p53 (Table 1). Interestingly, magnolin sensitivity on the cell proliferation was obverted in TOV-112D without alteration of SASP markers (Figure 4D), indicated that magnolin-mediated senescence is cellular senescence that is associated with cell cycle arrest (Figure 2A). In contrast, we further observed that magnolin induced the protein levels of p16[Ink4a] and p27[Kip1], critical markers for cellular senescence, in xenograft tissues (Figure 5E). Unfortunately, we could detect the SA-β-gal activity in tumor tissues because the tissues were fixed in 4% formalin for long period. These results suggest that constitutive active mutation in MAPK and PI3 K signaling pathways have a key role in bypassing cellular senescence.

Recently, genomic analysis of ovarian carcinoma indicated that *TP53* mutations are observed about 96% of high-grade serious ovarian cancers.[48] They also found additional somatic mutations in genes, including NF1, BRACA1, BRCA2, RB1, and CDK12, with low

prevalence but statistically recurrence.[48] The somatic mutations of BRCA1 and 2 are associated with other genes that are involved in DNA repair in high-grade ovarian cancers.[48] However, high-grade ovarian cancer are associated with about 10–20% germline mutations in BRCA1 and 2,[49] indicated that tumor suppressors plays a key role in ovarian cancer development. Moreover, it is clear that constitutive active mutations in MAPK signaling pathway was observed about each 11% of total epithelial ovarian cancers in B-Raf and K-Ras genes, respectively.[50] On the other hand, constitutive active mutation of PI3 K (PI3KCA) and loss-of-function of PTEN was observed with about 6.7 and 20% of the total epithelial ovarian cancers.[50,51] Analysis of the CCLE mutaome data has indicated that SKOV3 cells contain a constitutively active mutation in PI3 K and loss-of-function mutations in p16 and p53 (Table 1). Moreover, SKOV3 cell showed negative results following SA-β-gal staining and magnolin treatment, whereas, the opposite results were obtained with TOV-112D cells (Figure 4A). Importantly, we observed that the ovarian cancer cell marker CD44^{+}/CD24^{−} was enriched in sphere-formed SKOV3 cells, but not in sphere-formed TOV-112D cells (Figure 5A), thereby indicating that ERK1 and ERK2 targeting is suitable for the treatment of ovarian cancer cells that do not contain a constitutively active mutation in PI3 K and loss-of-function mutations in the p16 and p53 tumor suppressor proteins.

CONFLICT OF INTEREST

The authors declare no competing financial interest.

ORCID

Yong-Yeon Cho (iD) http://orcid.org/0000-0003-1107-2651

REFERENCES

1. Liu M, Chan D, Ngan H. Mechanisms of chemoresistance in human ovarian cancer at a glance. *Gynecol Obstet*. 2012;2:e104.
2. Siegel RL, Miller KD, Jemal A. Cancer statistics, 2015. *CA Cancer J Clin*. 2015;65:5–29.
3. Brachova P, Thiel KW, Leslie KK. The consequence of oncomorphic TP53 mutations in ovarian cancer. *Int J Mol Sci*. 2013;14: 19257–19275.
4. Holford J, Rogers P, Kelland LR. Ras mutation and platinum resistance in human ovarian carcinomas in vitro. *Int J Cancer*. 1998;77:94–100.
5. Steelman LS, Chappell WH, Abrams SL, et al. Roles of the Raf/MEK/ERK and PI3K/PTEN/Akt/mTOR pathways in controlling growth and sensitivity to therapy-implications for cancer and aging. *Aging (Albany NY)*. 2011;3:192–222.

6. McCubrey JA, Steelman LS, Chappell WH, et al. Ras/Raf/MEK/ERK and PI3K/PTEN/Akt/mTOR cascade inhibitors: how mutations can result in therapy resistance and how to overcome resistance. *Oncotarget*. 2012;3:1068–1111.
7. Jin W, Wu L, Liang K, Liu B, Lu Y, Fan Z. Roles of the PI-3K and MEK pathways in Ras-mediated chemoresistance in breast cancer cells. *Br J Cancer*. 2003;89:185–191.
8. Macerelli M, Caramella C, Faivre L, et al. Does KRAS mutational status predict chemoresistance in advanced non-small cell lung cancer (NSCLC)? *Lung Cancer*. 2014;83:383–388.
9. Arcaro A, Guerreiro AS. The phosphoinositide 3-kinase pathway in human cancer: genetic alterations and therapeutic implications. *Curr Genomics*. 2007;8:271–306.
10. Yang L, Zhou Y, Li Y, et al. Mutations of p53 and KRAS activate NF-kappaB to promote chemoresistance and tumorigenesis via dysregulation of cell cycle and suppression of apoptosis in lung cancer cells. *Cancer Lett*. 2015;357:520–526.
11. McCubrey JA, Steelman LS, Kempf CR, et al. Therapeutic resistance resulting from mutations in Raf/MEK/ERK and PI3K/PTEN/Akt/mTOR signaling pathways. *J Cell Physiol*. 2011;226:2762–2781.
12. Wang Z, Martin D, Molinolo AA, et al. MTOR co-targeting in cetuximab resistance in head and neck cancers harboring PIK3CA and RAS mutations. *J Natl Cancer Inst*. 2014;106.
13. Lee CJ, Lee HS, Ryu HW, et al. Targeting of magnolin on ERKs inhibits Ras/ERKs/RSK2-signaling-mediated neoplastic cell transformation. *Carcinogenesis*. 2014;35:432–441.
14. Seiler AE, Spielmann H. The validated embryonic stem cell test to predict embryotoxicity in vitro. *Nat Protoc*. 2011;6:961–978.
15. Cho YY. RSK2 and its binding partners in cell proliferation, transformation and cancer development. *Arch Pharm Res*. 2017;40: 291–303.
16. Cho YY. Molecular targeting of ERKs/RSK2 signaling in cancers. *Curr Pharm Des*. 2017;23:4247–4258.
17. Roberts PJ, Der CJ. Targeting the Raf-MEK-ERK mitogen-activated protein kinase cascade for the treatment of cancer. *Oncogene*. 2007;26:3291–3310.
18. Liu K, Cho YY, Yao K, et al. Eriodictyol inhibits RSK2-ATF1 signaling and suppresses EGF-induced neoplastic cell transformation. *J Biol Chem*. 2011;286:2057–2066.
19. Rodier F, Campisi J. Four faces of cellular senescence. *J Cell Biol*. 2011;192:547–556.
20. Cho YY, Yao K, Kim HG, et al. Ribosomal S6 kinase 2 is a key regulator in tumor promoter induced cell transformation. *Cancer Res*. 2007;67:8104–8112.
21. Chien Y, Scuoppo C, Wang X, et al. Control of the senescence-associated secretory phenotype by NF-kappaB promotes senescence and enhances chemosensitivity. *Genes Dev*. 2011;25:2125–2136.
22. Lee CJ, Lee MH, Yoo SM, et al. Magnolin inhibits cell migration and invasion by targeting the ERKs/RSK2 signaling pathway. *BMC Cancer*. 2015;15:576.
23. Coppe JP, Desprez PY, Krtolica A, Campisi J. The senescence-associated secretory phenotype: the dark side of tumor suppression. *Annu Rev Pathol*. 2010;5:99–118.
24. Vinogradov S, Wei X. Cancer stem cells and drug resistance: the potential of nanomedicine. *Nanomedicine (Lond)*. 2012;7:597–615.
25. Jaggupilli A, Elkord E. Significance of CD44 and CD24 as cancer stem cell markers: an enduring ambiguity. *Clin Dev Immunol*. 2012;2012:708036.
26. Meng E, Long B, Sullivan P, et al. CD44+/CD24- ovarian cancer cells demonstrate cancer stem cell properties and correlate to survival. *Clin Exp Metastasis*. 2012;29:939–948.
27. Mendoza MC, Er EE, Blenis J. The Ras-ERK and PI3K-mTOR pathways: cross-talk and compensation. *Trends Biochem Sci*. 2011;36:320–328.
28. Sim S, Kacevska M, Ingelman-Sundberg M. Pharmacogenomics of drug-metabolizing enzymes: a recent update on clinical implications and endogenous effects. *Pharmacogenomic J* 2013;13:1–11.

29. Rivlin N, Brosh R, Oren M, Rotter V. Mutations in the p53 tumor suppressor gene: important milestones at the various steps of tumorigenesis. *Genes Cancer*. 2011;2:466–474.

30. Ben-Porath I, Weinberg RA. The signals and pathways activating cellular senescence. *Int J Biochem Cell Biol*. 2005;37:961–976.

31. Boja ES, Rodriguez H. Proteogenomic convergence for understanding cancer pathways and networks. *Clin Proteomics*. 2014;11:22.

32. Holohan C, Van Schaeybroeck S, Longley DB, Johnston PG. Cancer drug resistance: an evolving paradigm. *Nat Rev Cancer*. 2013;13: 714–726.

33. Housman G, Byler S, Heerboth S, et al. Drug resistance in cancer: an overview. *Cancers*. 2014;6:1769–1792.

34. Aksamitiene E, Kiyatkin A, Kholodenko BN. Cross-talk between mitogenic Ras/MAPK and survival PI3K/Akt pathways: a fine balance. *Biochem Soc Trans*. 2012;40:139–146.

35. Mitchell R, Kumar V, Abbas A, Aster J. *Pocket companion to Robbins & Cotran pathologic basis of disease*. 8th ed. Philadelphia, United Kingdom: Elsevier Health Science; 2011.

36. Hanahan D, Weinberg RA. Hallmarks of cancer: the next generation. *Cell*. 2011;144:646–674.

37. Walsh JH, Karnes WE, Cuttitta F, Walker A. Autocrine growth factors and solid tumor malignancy. *West J Med*. 1991;155:152–163.

38. Loeb KR, Loeb LA. Significance of multiple mutations in cancer. *Carcinogenesis*. 2000;21:379–385.

39. Jang S, Atkins MB. Which drug, and when, for patients with BRAF-mutant melanoma? *Lancet. Oncol* 2013;14:e60–e69.

40. Samuels Y, Wang Z, Bardelli A, et al. High frequency of mutations of the PIK3CA gene in human cancers. *Science*. 2004;304:554.

41. Testa JR, Tsichlis PN. AKT signaling in normal and malignant cells. *Oncogene*. 2005;24:7391–7393.

42. Gaglio D, Metallo CM, Gameiro PA, et al. Oncogenic K-Ras decouples glucose and glutamine metabolism to support cancer cell growth. *Mol Syst Biol*. 2011;7:523.

43. Yu M, Grady WM. Therapeutic targeting of the phosphatidylinositol 3-kinase signaling pathway: novel targeted therapies and advances in the treatment of colorectal cancer. *Therap Adv Gastroenterol*. 2012;5:319–337.

44. Gordon RR, Nelson PS. Cellular senescence and cancer chemotherapy resistance. *Drug Resist Updat*. 2012;15:123–131.

45. Wei W, Herbig U, Wei S, Dutriaux A, Sedivy JM. Loss of retinoblastoma but not p16 function allows bypass of replicative senescence in human fibroblasts. *EMBO Rep*. 2003;4:1061–1066.

46. Chen Z, Trotman LC, Shaffer D, et al. Crucial role of p53-dependent cellular senescence in suppression of Pten-deficient tumorigenesis. *Nature*. 2005;436:725–730.

47. Sarkisian CJ, Keister BA, Stairs DB, Boxer RB, Moody SE, Chodosh LA. Dose-dependent oncogene-induced senescence in vivo and its evasion during mammary tumorigenesis. *Nat Cell Biol*. 2007;9: 493–505.

48. Cancer Genome Atlas Research N. Integrated genomic analyses of ovarian carcinoma. *Nature*. 2011;474:609–615.

49. Pal T, Permuth-Wey J, Betts JA, et al. BRCA1 and BRCA2 mutations account for a large proportion of ovarian carcinoma cases. *Cancer*. 2005;104:2807–2816.

50. Kurman RJ, Shih Ie M. Molecular pathogenesis and extraovarian origin of epithelial ovarian cancer--shifting the paradigm. *Hum Pathol*. 2011;42:918–931.

51. Campbell IG, Russell SE, Phillips WA. PIK3CA mutations in ovarian cancer. *Clin Cancer Res*. 2005;11:7042–7043; author reply 7042–7043.

SUPPORTING INFORMATION

Additional supporting information may be found online in the Supporting Information section at the end of the article.